PH 208: Lecture Notes on Ferromagnetism

Aveek Bid

Contents

1 Introduction

Ferromagnetism is the phenomenon in which a material exhibits a spontaneous magnetization below a critical temperature known as the Curie temperature T_C. In the ferromagnetic phase, the magnetic moments of electrons align parallel to each other even in the absence of an applied magnetic field.

Examples of elemental ferromagnets include Fe, Co, and Ni. Ferromagnetism arises from quantum mechanical exchange interactions between electron spins and cannot be explained by classical magnetic dipole interactions alone.

The central questions addressed in the theory of ferromagnetism are:

- Why do electron spins align spontaneously?

- What microscopic interactions produce this alignment?
- How does magnetization depend on temperature?
- What are the elementary excitations of a ferromagnet?

2 Magnetic Moment of Electrons

The magnetic moment of an electron has contributions from both orbital and spin angular momentum.
Orbital magnetic moment:

$$\boldsymbol{\mu}_L = -\mu_B \frac{\mathbf{L}}{\hbar} \tag{1}$$

and, spin magnetic moment:

$$\boldsymbol{\mu}_S = -g_s \mu_B \frac{\mathbf{S}}{\hbar} \tag{2}$$

where, $\mu_B = \frac{e\hbar}{2m}$ is the Bohr magneton.

In most transition metals, the orbital moment is largely quenched by the crystal field, and magnetism arises primarily from electron spin (see Appendix A).

3 Failure of Classical Dipole Interaction

A naive explanation of ferromagnetism might invoke magnetic dipole interactions.
The dipole-dipole interaction energy is approximately.

$$E_{dd} \sim \frac{\mu_0}{4\pi} \frac{\mu^2}{r^3} \tag{3}$$

Using typical atomic parameters

$$\mu \sim \mu_B, \qquad r \sim 3\,\text{Å}$$

gives

$$E_{dd} \sim 10^{-4}\,\text{eV}$$

However, the Curie temperature corresponds to energies

$$k_B T_C \sim 0.1\,\text{eV}$$

Thus, classical dipole interactions are far too weak to explain ferromagnetism.

4 Exchange Interaction

The fundamental origin of ferromagnetism is the **exchange interaction**. This purely quantum mechanical effect arises from the combination of the Coulomb interaction and the antisymmetry of the electronic wavefunction required by the Pauli exclusion principle.

4.1 Two-electron system

To understand the origin of exchange, consider two interacting electrons in an external potential $V(\mathbf{r})$. The Hamiltonian is

$$H = \frac{p_1^2}{2m} + \frac{p_2^2}{2m} + V(\mathbf{r}_1) + V(\mathbf{r}_2) + \frac{e^2}{|\mathbf{r}_1 - \mathbf{r}_2|} \tag{4}$$

Because electrons are fermions, the total wavefunction must be antisymmetric under particle exchange,

$$\Psi(1,2) = -\Psi(2,1). \tag{5}$$

The total wavefunction can be written as a product of spatial and spin parts,

$$\Psi = \psi(\mathbf{r}_1, \mathbf{r}_2)\chi(s_1, s_2). \tag{6}$$

The antisymmetry requirement implies that if the spin wavefunction is symmetric, the spatial wavefunction must be antisymmetric, and vice versa.

4.2 Singlet and triplet states

Two distinct spin configurations are therefore possible.
Singlet state. The spin wavefunction is antisymmetric,

$$\chi_s = \frac{1}{\sqrt{2}}(\uparrow\downarrow - \downarrow\uparrow), \tag{7}$$

So the spatial wavefunction must be symmetric,

$$\psi_s(\mathbf{r}_1, \mathbf{r}_2) = \frac{1}{\sqrt{2}}\left[\phi_a(\mathbf{r}_1)\phi_b(\mathbf{r}_2) + \phi_a(\mathbf{r}_2)\phi_b(\mathbf{r}_1)\right]. \tag{8}$$

Triplet state. The spin wavefunction is symmetric,

$$\chi_{t1} = \uparrow\uparrow \tag{9}$$

$$\chi_{t0} = \frac{1}{\sqrt{2}}(\uparrow\downarrow + \downarrow\uparrow) \tag{10}$$

$$\chi_{t-1} = \downarrow\downarrow, \tag{11}$$

and therefore the spatial wavefunction must be antisymmetric,

$$\psi_t(\mathbf{r}_1, \mathbf{r}_2) = \frac{1}{\sqrt{2}}\left[\phi_a(\mathbf{r}_1)\phi_b(\mathbf{r}_2) - \phi_a(\mathbf{r}_2)\phi_b(\mathbf{r}_1)\right]. \tag{12}$$

4.3 Direct and exchange Coulomb integrals

The expectation value of the Coulomb interaction

$$V_C = \frac{e^2}{|\mathbf{r}_1 - \mathbf{r}_2|}$$

contains two distinct contributions.

Direct Coulomb integral

$$J_D = \int d^3r_1 d^3r_2 |\phi_a(\mathbf{r}_1)|^2 |\phi_b(\mathbf{r}_2)|^2 \frac{e^2}{|\mathbf{r}_1 - \mathbf{r}_2|}, \tag{13}$$

which corresponds to the classical electrostatic interaction between the two charge distributions.
Exchange integral

$$J = \int d^3r_1 d^3r_2 \phi_a^*(\mathbf{r}_1)\phi_b^*(\mathbf{r}_2) \frac{e^2}{|\mathbf{r}_1 - \mathbf{r}_2|} \phi_a(\mathbf{r}_2)\phi_b(\mathbf{r}_1). \tag{14}$$

This term has no classical analogue and arises entirely from the quantum-mechanical symmetry of the electronic wavefunction.

4.4 Energy splitting

Evaluating the expectation value of the Hamiltonian gives

$$E_{\text{singlet}} = E_0 + J_D + J, \tag{15}$$
$$E_{\text{triplet}} = E_0 + J_D - J. \tag{16}$$

The energy difference between the two states is therefore

$$E_{\text{singlet}} - E_{\text{triplet}} = 2J. \tag{17}$$

This energy splitting can be written in the form of an effective spin Hamiltonian,

$$H_{ex} = -2J\, \mathbf{S}_1 \cdot \mathbf{S}_2. \tag{18}$$

If $J > 0$, the triplet state is lower in energy and parallel spin alignment is favored, leading to ferromagnetism. If $J < 0$, the singlet state is favored, resulting in antiferromagnetic coupling.

4.5 Physical interpretation of exchange

Although the exchange integral contains no explicit spin variables, it produces an effective interaction between spins because the symmetry of the spin wavefunction determines the symmetry of the spatial wavefunction.
For parallel spins (triplet state), the spatial wavefunction is antisymmetric. In particular,

$$\psi_t(\mathbf{r}, \mathbf{r}) = 0,$$

which means that two electrons with the same spin cannot occupy the same spatial position. As a result, electrons with parallel spins tend to avoid each other, reducing their Coulomb repulsion.
This reduction in Coulomb energy relative to the singlet state is the **exchange energy**. The exchange interaction, therefore, originates from the modification of electron spatial correlations imposed by the Pauli principle. It is not a classical magnetic interaction between spins but a purely quantum mechanical consequence of electron indistinguishability.

The magnitude of the exchange integral depends strongly on the overlap of the electronic orbitals. If the orbitals on neighboring sites overlap weakly, the exchange interaction becomes small. Consequently, exchange interactions in solids are typically short ranged and act primarily between nearest neighbors.

4.6 The exchange hole picture

A particularly intuitive way to understand exchange is through the concept of the **exchange hole**. The key idea is that an electron with a given spin reduces the probability of finding another electron with the same spin nearby.
Consider placing an electron with spin up at position $\mathbf{r}_0$. Because the spatial wavefunction for two electrons with parallel spins is antisymmetric, the probability of finding another spin-up electron close to $\mathbf{r}_0$ is reduced. In fact,

$$\psi(\mathbf{r}, \mathbf{r}) = 0$$

for identical spins. This creates a region around the electron in which the density of same-spin electrons is suppressed. This region is called the exchange hole.
The exchange hole affects only electrons with the same spin; electrons with opposite spin are not subject to the same Pauli constraint. Because the exchange hole pushes same-spin electrons apart, the average separation between electrons increases, reducing the Coulomb repulsion

$$E_C = \frac{e^2}{|\mathbf{r}_1 - \mathbf{r}_2|}. \tag{19}$$

The resulting reduction in Coulomb energy is the physical origin of the exchange interaction. If many electrons align their spins, the exchange hole operates collectively between many pairs of electrons, and the total Coulomb energy of the system decreases. In this way, the system can lower its energy through spin alignment, providing an intuitive explanation of Hund's rule and the tendency toward ferromagnetism in itinerant-electron systems.
The spatial extent of the exchange hole in metals is typically of the order

$$\sim k_F^{-1}, \tag{20}$$

where k_F is the Fermi wavevector, the exchange hole has no classical analogue and arises entirely from the fermionic statistics of electrons.

4.7 Connection to the Heisenberg Hamiltonian

In a crystal with many localized magnetic moments, the exchange interaction between pairs of spins leads to the Heisenberg model

$$H = -\sum_{ij} J_{ij} \mathbf{S}_i \cdot \mathbf{S}_j \tag{21}$$

where J_{ij} depends on the overlap of the electronic orbitals on sites i and j. This effective Hamiltonian forms the basis of the theoretical description of magnetically ordered materials.

5 Heisenberg Model

At energies much smaller than the electronic excitation energies, the microscopic Coulomb interaction between electrons can be replaced by an effective interaction between localized spins. The resulting effective Hamiltonian is the **Heisenberg Hamiltonian**,

$$H = -\sum_{i,j} J_{ij}\, \mathbf{S}_i \cdot \mathbf{S}_j. \tag{22}$$

Here $\mathbf{S}_i$ denotes the spin operator associated with the magnetic moment on lattice site i, and J_{ij} is the exchange coupling between spins on sites i and j. The sign and magnitude of J_{ij} depend on the overlap of the electronic orbitals and the microscopic exchange mechanisms present in the material.
The scalar product of spin operators may be written as

$$\mathbf{S}_i \cdot \mathbf{S}_j = S_i^x S_j^x + S_i^y S_j^y + S_i^z S_j^z. \tag{23}$$

This interaction is rotationally invariant in spin space, reflecting the fact that in the absence of spin–orbit coupling, the exchange interaction does not select a preferred spin direction.

5.1 Nearest-neighbour approximation

In most solids, the exchange interaction decreases rapidly with distance because it depends sensitively on orbital overlap. It is therefore often sufficient to retain only nearest-neighbour interactions,

$$H = -J \sum_{\langle ij \rangle} \mathbf{S}_i \cdot \mathbf{S}_j, \tag{24}$$

where $\langle ij \rangle$ denotes pairs of nearest-neighbour lattice sites.

5.2 Ground states

The nature of the ground state depends on the sign of the exchange constant J.

- **Ferromagnetic coupling ($J > 0$).** The energy is minimized when neighbouring spins align parallel to each other. The ground state corresponds to all spins pointing in the same direction, producing a macroscopic magnetization.
- **Antiferromagnetic coupling ($J < 0$).** The energy is minimized when neighbouring spins are antiparallel. On a bipartite lattice, this produces the **Néel state**, in which the lattice divides into two sublattices with opposite spin orientations.

For the ferromagnetic case, the classical ground state may be written as

$$\mathbf{S}_1 = \mathbf{S}_2 = \cdots = \mathbf{S}_N,$$

meaning that all spins are aligned. Because the Hamiltonian is rotationally invariant, the direction of the common spin orientation is arbitrary. This degeneracy reflects the continuous spin-rotation symmetry of the system. Hence, small deviations cost zero energy - this leads to spin waves.

5.3 Physical significance

Despite its apparent simplicity, the Heisenberg model captures many essential features of magnetic materials, including

- ferromagnetic and antiferromagnetic order,
- collective spin excitations (spin waves),
- magnetic phase transitions.

The Heisenberg model, therefore, provides the starting point for the theoretical description of magnetism in solids.

6 Spin Waves in the Heisenberg Ferromagnet

The ground state of a ferromagnet corresponds to all spins aligned parallel. Small deviations from this ordered state propagate through the lattice as collective excitations known as **spin waves**. The deviated spins precess due to the torque on them from the other spins. The quanta of these excitations are called **magnons**. Each magnon reduces the total magnetization by one unit of $\hbar$. Introducing spin raising and lowering operators

$$S_i^+ = S_i^x + iS_i^y \tag{25}$$
$$S_i^- = S_i^x - iS_i^y, \tag{26}$$

the Heisenberg Hamiltonian becomes

$$H = -J \sum_{\langle ij \rangle} \left(S_i^z S_j^z + \frac{1}{2} S_i^+ S_j^- + \frac{1}{2} S_i^- S_j^+ \right). \tag{27}$$

Using the Holstein–Primakoff transformation

$$S_i^+ = \sqrt{2S}\, a_i \tag{28}$$
$$S_i^- = \sqrt{2S}\, a_i^\dagger \tag{29}$$
$$S_i^z = S - a_i^\dagger a_i, \tag{30}$$

and retaining terms to leading order in magnon density yields

$$H = E_0 + \sum_k \epsilon(k) a_k^\dagger a_k. \tag{31}$$

The magnon dispersion relation is

$$\epsilon(k) = 2JSz(1 - \gamma_k), \tag{32}$$

where

$$\gamma_k = \frac{1}{z} \sum_\delta e^{ik \cdot \delta}. \tag{33}$$

The sum runs over all nearest-neighbor vectors δ connecting a lattice site to its neighboring sites, and z is the coordination number of the lattice.

6.1 Long-wavelength limit

For $ka \ll 1$ we obtain

$$\epsilon(k) \approx Dk^2, \tag{34}$$

where

$$D = JSa^2 \tag{35}$$

is the **spin stiffness**. Thus, ferromagnetic magnons exhibit a **quadratic dispersion**.

6.2 Bloch's $T^{3/2}$ Law

Thermal excitation of magnons reduces the magnetization of a ferromagnet. The number of thermally excited magnons is

$$N_m = \frac{V}{(2\pi)^3} \int \frac{d^3k}{e^{\epsilon(k)/k_B T} - 1}. \tag{36}$$

For ferromagnets $\epsilon(k) = Dk^2$, which leads to

$$N_m \propto T^{3/2}. \tag{37}$$

Since each magnon reduces the magnetization by one unit of spin,

$$M(T) = M(0) - AT^{3/2}. \tag{38}$$

This result is known as **Bloch's $T^{3/2}$ law**.

7 Spin Waves in Heisenberg Antiferromagnets

7.1 Linear magnon dispersion in antiferromagnets

The dispersion relation of spin waves in antiferromagnets differs qualitatively from that of ferromagnets. In a ferromagnet, the magnon dispersion is quadratic ($\epsilon_k \propto k^2$), whereas in an antiferromagnet it is linear ($\epsilon_k \propto k$) at long wavelengths. To demonstrate this result, we consider the nearest-neighbour Heisenberg antiferromagnet

$$H = -J \sum_{\langle ij \rangle} \mathbf{S}_i \cdot \mathbf{S}_j, \tag{39}$$

with $J < 0$.

Néel ground state

On a bipartite lattice, the classical ground state is the Néel state in which spins on the two sublattices point in opposite directions:

$$\mathbf{S}_i = S\hat{z} \quad (i \in A), \qquad \mathbf{S}_j = -S\hat{z} \quad (j \in B).$$

Because the two sublattices have opposite orientations, we introduce separate bosonic operators for the two sublattices using the Holstein–Primakoff transformation.
For sublattice A

$$S_i^z = S - a_i^\dagger a_i \tag{40}$$

$$S_i^+ = \sqrt{2S}\, a_i \tag{41}$$

$$S_i^- = \sqrt{2S}\, a_i^\dagger \tag{42}$$

For sublattice B

$$S_j^z = -S + b_j^\dagger b_j \tag{43}$$
$$S_j^+ = \sqrt{2S}\, b_j^\dagger \tag{44}$$
$$S_j^- = \sqrt{2S}\, b_j. \tag{45}$$

Linear spin-wave Hamiltonian

Substituting these expressions into the Heisenberg Hamiltonian and retaining only terms quadratic in the boson operators yields

$$H = E_0 + JS \sum_{\langle ij \rangle} \left(a_i^\dagger a_i + b_j^\dagger b_j + a_i b_j + a_i^\dagger b_j^\dagger \right). \tag{46}$$

We now perform the Fourier transform

$$a_i = \frac{1}{\sqrt{N}} \sum_k a_k e^{ik \cdot r_i} \tag{47}$$
$$b_j = \frac{1}{\sqrt{N}} \sum_k b_k e^{ik \cdot r_j}. \tag{48}$$

The Hamiltonian becomes

$$H = E_0 + JSz \sum_k \left[a_k^\dagger a_k + b_k^\dagger b_k + \gamma_k (a_k b_{-k} + a_k^\dagger b_{-k}^\dagger) \right], \tag{49}$$

where z is the coordination number and

$$\gamma_k = \frac{1}{z} \sum_\delta e^{ik \cdot \delta}. \tag{50}$$

Diagonalization

The Hamiltonian can be diagonalized using a Bogoliubov transformation. The resulting magnon spectrum is

$$\epsilon(k) = JSz\sqrt{1 - \gamma_k^2}. \tag{51}$$

Long wavelength limit

For small wavevectors ($ka \ll 1$) we expand

$$\gamma_k \approx 1 - \frac{a^2 k^2}{2}. \tag{52}$$

Substituting into the dispersion relation gives

$$\epsilon(k) \approx JSz\sqrt{1 - \left(1 - \frac{a^2 k^2}{2}\right)^2} \tag{53}$$
$$\approx JSz\, ak. \tag{54}$$

Thus, the long-wavelength magnon dispersion is

$$\epsilon(k) = ck, \tag{55}$$

where

$$c = JSza \tag{56}$$

is the **spin-wave velocity**.

Physical interpretation

The linear dispersion arises because the antiferromagnetic ground state contains two oppositely oriented sublattices. A disturbance of one sublattice immediately affects the other, producing a propagating collective mode analogous to an acoustic wave.

7.2 Low-temperature magnetization in antiferromagnets

For antiferromagnets, the magnon dispersion is linear,

$$\epsilon(k) \propto k.$$

Repeating the same analysis gives

$$N_m \propto T^3 \tag{57}$$

and therefore

$$M(T) = M(0) - BT^3. \tag{58}$$

7.3 Origin of the different temperature dependences

The difference arises from the long-wavelength magnon dispersion:

System	Dispersion	Magnetization correction
Ferromagnet	$\epsilon(k) \propto k^2$	$T^{3/2}$
Antiferromagnet	$\epsilon(k) \propto k$	T^3

Thus, the temperature dependence of the magnetization is directly determined by the dispersion relation of the spin-wave excitations.

8 Weiss Mean Field Theory

A major step toward understanding ferromagnetism was made by Weiss, who introduced the concept of a **molecular field**. The central idea is that each magnetic moment experiences not only the externally applied magnetic field but also an additional internal field produced by neighboring moments.
Weiss proposed that this internal field is proportional to the magnetization of the material. The effective magnetic field acting on a spin is therefore

$$B_{\text{eff}} = B + \lambda M, \tag{59}$$

where B is the external magnetic field, M is the magnetization, and λ is the **molecular field constant**. This phenomenological relation incorporates the effect of the exchange interaction in an average way.

8.1 Magnetization of localized spins

Consider a system of N localized spins of magnitude S. In an effective magnetic field B_{eff}, the magnetization is given by

$$M = Ng\mu_B S B_S(x), \tag{60}$$

where g is the Landé g-factor, μ_B is the Bohr magneton, and $B_S(x)$ is the **Brillouin function**,

$$B_S(x) = \frac{2S+1}{2S}\coth\left(\frac{2S+1}{2S}x\right) - \frac{1}{2S}\coth\left(\frac{x}{2S}\right). \tag{61}$$

The argument of the Brillouin function is

$$x = \frac{g\mu_B S B_{\text{eff}}}{k_B T}. \tag{62}$$

Substituting the expression for the effective field gives the **self-consistency equation**

$$M = Ng\mu_B S B_S\left(\frac{g\mu_B S(B+\lambda M)}{k_B T}\right). \tag{63}$$

This equation determines the magnetization as a function of temperature and applied magnetic field.

8.2 Curie temperature

Spontaneous magnetization corresponds to a nonzero solution for M even when the external field $B = 0$. To determine the transition temperature we consider the limit of small magnetization near the critical point.
For small x, the Brillouin function can be expanded as

$$B_S(x) \approx \frac{S+1}{3S}x. \tag{64}$$

Substituting this approximation into the self-consistency equation with $B = 0$ gives

$$M = Ng\mu_B S\left(\frac{S+1}{3S}\right)\frac{g\mu_B S\lambda M}{k_B T}. \tag{65}$$

Cancelling M yields the condition

$$1 = \frac{Ng^2\mu_B^2 S(S+1)}{3k_B T_C}\lambda. \tag{66}$$

The temperature at which this equality holds defines the **Curie temperature**

$$T_C = \frac{Ng^2\mu_B^2 S(S+1)}{3k_B}\lambda. \tag{67}$$

Below this temperature the system develops spontaneous magnetization.

8.3 Curie–Weiss law

Above the Curie temperature, the magnetization is small and proportional to the applied field. Linearizing the self-consistency equation yields

$$M = \chi B, \tag{68}$$

where the magnetic susceptibility becomes

$$\chi = \frac{C}{T - T_C}. \tag{69}$$

Here

$$C = \frac{N g^2 \mu_B^2 S(S+1)}{3 k_B} \tag{70}$$

is the **Curie constant**. This result is known as the **Curie–Weiss law**.

8.4 Physical interpretation

Weiss mean field theory predicts that the exchange interaction produces an internal molecular field that reinforces the alignment of spins. When the temperature is sufficiently low, this internal field is strong enough to maintain spin alignment even in the absence of an external magnetic field, leading to spontaneous magnetization.

Although Weiss theory successfully explains the Curie–Weiss law and the existence of a phase transition, it neglects fluctuations of the spin system. As a result it overestimates the Curie temperature and predicts mean-field critical exponents. Nevertheless, it provides an important conceptual framework for understanding magnetic phase transitions.

8.5 Connection to the Heisenberg exchange interaction

The molecular field introduced by Weiss can be understood microscopically by starting from the Heisenberg Hamiltonian

$$H = -J \sum_{\langle ij \rangle} \mathbf{S}_i \cdot \mathbf{S}_j, \tag{71}$$

where J is the exchange constant and the sum runs over nearest-neighbour pairs.
In the mean-field approximation, each spin is assumed to interact with the *average* magnetization of its neighbors rather than their instantaneous fluctuating orientations. Writing the spin operator as

$$\mathbf{S}_j = \langle \mathbf{S}_j \rangle + (\mathbf{S}_j - \langle \mathbf{S}_j \rangle),$$

and neglecting the fluctuation term, we obtain

$$\mathbf{S}_i \cdot \mathbf{S}_j \approx \mathbf{S}_i \cdot \langle \mathbf{S}_j \rangle. \tag{72}$$

If each lattice site has z nearest neighbours, the Hamiltonian acting on spin i becomes

$$H_i \approx -Jz\, \mathbf{S}_i \cdot \langle \mathbf{S} \rangle. \tag{73}$$

The magnetization per unit volume is related to the average spin by

$$M = ng\mu_B\langle S_z\rangle, \tag{74}$$

where n is the number density of spins.
Thus the mean-field Hamiltonian can be written as

$$H_i = -g\mu_B \mathbf{S}_i \cdot \mathbf{B}_{\mathrm{mf}}, \tag{75}$$

where the effective molecular field is

$$B_{\mathrm{mf}} = \frac{2zJ}{(g\mu_B)^2} M. \tag{76}$$

Comparing this expression with the Weiss assumption

$$B_{\mathrm{eff}} = B + \lambda M, \tag{77}$$

we identify the molecular field constant as

$$\lambda = \frac{2zJ}{(g\mu_B)^2}. \tag{78}$$

8.6 Curie temperature in terms of exchange

Substituting this result into the Weiss expression for the Curie temperature gives

$$T_C = \frac{2zJ}{3k_B} S(S+1). \tag{79}$$

This relation shows that the Curie temperature is determined by the strength of the exchange interaction and the number of nearest neighbours. Stronger exchange coupling and larger coordination number both increase the ordering temperature.

8.7 Physical interpretation

The Weiss molecular field is therefore not a real magnetic field but rather an effective field arising from exchange interactions with neighboring spins. In the mean-field approximation each spin experiences an average field produced by the surrounding magnetization, which tends to align it parallel to the existing magnetic order.
This derivation demonstrates that Weiss mean-field theory can be viewed as the mean-field approximation to the Heisenberg model. The phenomenological parameter λ is directly related to the microscopic exchange constant J.

8.8 Validity and limitations of mean-field theory

Weiss mean-field theory provides a remarkably simple description of ferromagnetism and successfully explains several important experimental observations, including the Curie–Weiss law and the existence of a ferromagnetic phase transition. Nevertheless, the theory relies on a strong approximation: each spin is assumed to interact only with the *average* magnetization of its neighbors, while fluctuations of the local spin configuration are neglected.
The accuracy of this approximation depends strongly on the dimensionality of the system and on the number of interacting neighbors.

Role of coordination number

In a lattice with coordination number z, each spin interacts with z neighbors. When z is large, the fluctuations in the local environment of a spin tend to average out, making the mean-field approximation more accurate. In this sense, mean-field theory becomes exact in the limit of infinite coordination number.
This explains why Weiss theory often gives a reasonable estimate of the Curie temperature in three-dimensional magnetic materials.

Importance of fluctuations

Near the critical temperature T_C, fluctuations of the magnetization become large and long-ranged. These fluctuations are not captured by mean-field theory, which assumes a spatially uniform magnetization. As a result, Weiss theory predicts incorrect critical exponents for the magnetic phase transition.
For example, mean-field theory predicts that the spontaneous magnetization near T_C behaves as

$$M(T) \propto (T_C - T)^{1/2}, \tag{80}$$

corresponding to a critical exponent $\beta = 1/2$. In real materials, however, experiments typically find smaller values, such as

$$\beta \approx 0.33$$

for three-dimensional Heisenberg magnets.

Effect of dimensionality

The importance of fluctuations increases dramatically in lower dimensions. In fact, the Mermin–Wagner theorem shows that continuous spin-rotation symmetry cannot be spontaneously broken at finite temperature in one- or two-dimensional systems with short-range interactions.
As a consequence:

- One-dimensional Heisenberg magnets do not exhibit long-range magnetic order at finite temperature.
- Two-dimensional isotropic Heisenberg magnets also lack long-range order at finite temperature.

Thus mean-field theory greatly overestimates the tendency toward magnetic ordering in low-dimensional systems.

Summary

Despite its limitations, Weiss mean-field theory remains extremely important because it captures the essential physics of magnetic ordering in a simple framework. More sophisticated approaches, such as renormalization-group theory and numerical simulations, are required to describe the critical behavior near the transition temperature.

9 Ferromagnetic Hysteresis

One of the most characteristic experimental signatures of ferromagnetism is the existence of **magnetic hysteresis**. When an external magnetic field is applied and cycled, the magnetization does not follow the same path during increasing and decreasing field. Instead, the system exhibits a history-dependent response, forming a closed loop known as the **hysteresis loop**.

9.1 Basic phenomenology

Consider a ferromagnet initially in a demagnetized state. As the external magnetic field H is increased, the magnetization M increases and eventually saturates at a value M_s known as the **saturation magnetization**. If the field is now reduced to zero, the magnetization does not return to zero but instead retains a finite value M_r, called the **remanent magnetization**.
To reduce the magnetization to zero, a finite reverse field H_c must be applied. This field is called the **coercive field**. Continuing to increase the negative field leads to saturation in the opposite direction. Reversing the field again completes the hysteresis loop.

9.2 Hysteresis loop

The magnetization curve therefore forms a loop characterized by three important quantities:

- **Saturation magnetization** M_s: maximum magnetization at large field.
- **Remanence** M_r: magnetization at zero applied field.
- **Coercivity** H_c: field required to reduce M to zero.

The area enclosed by the hysteresis loop represents the **energy loss per cycle** due to irreversible processes in the material.

9.3 Origin of hysteresis: magnetic domains

The microscopic origin of hysteresis lies in the existence of **magnetic domains**. A uniformly magnetized crystal produces a large magnetostatic energy due to stray fields. To minimize this energy, the system breaks into domains within which the magnetization is uniform but oriented in different directions.
In zero applied field, domains are arranged so that the net magnetization is small or zero. When a magnetic field is applied, magnetization increases through two main processes:

1. **Domain wall motion**: domains aligned with the field grow at the expense of others.
2. **Domain rotation**: spins within domains gradually rotate toward the field direction.

These mechanisms dominate in different regions of the hysteresis curve.

(1) Initial magnetization: domain wall motion

Starting from a demagnetized state, the material consists of many domains with different orientations. As a small external field is applied, magnetization increases primarily through **domain wall motion**.

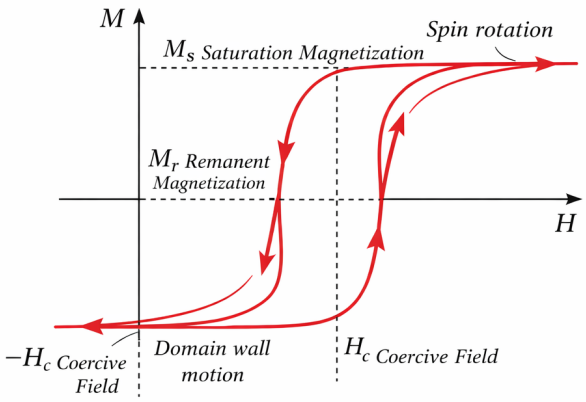

Figure 1: Origin of hysteresis in ferromagnets

Domains whose magnetization is aligned with the field grow at the expense of unfavorable domains. This process requires relatively little energy because it involves shifting domain boundaries rather than rotating all spins.
As a result:

- The initial part of the M–H curve is steep.
- Magnetization increases rapidly with small applied field.

This regime is largely reversible at very small fields but becomes irreversible once domain walls encounter pinning centers.

(2) Intermediate region: irreversible domain wall motion

As the field increases further, domain walls move through the crystal but are hindered by defects, impurities, and grain boundaries.
Overcoming these pinning centers requires finite energy, leading to:

- irreversible jumps in magnetization,
- hysteresis and energy loss.

This regime contributes significantly to the width of the hysteresis loop and to the coercive field.

(3) Approach to saturation: spin rotation

Once domains aligned with the field have grown to occupy most of the sample, further increase in magnetization cannot occur through domain wall motion. Instead, the magnetization increases through **rotation of spins within domains** toward the direction of the applied field.

This process involves overcoming magnetic anisotropy energy and is therefore more gradual. As a result:

- The M–H curve becomes less steep.
- Magnetization approaches saturation smoothly.

(4) Saturation regime

At large fields, all spins are nearly aligned with the field, and the system reaches the **saturation magnetization** M_s. Further increases in field produce negligible change in magnetization.

(5) Field reversal and coercivity

When the field is reduced from saturation, the reverse process does not retrace the same path because domain walls remain pinned.

- Initially, small changes are dominated by **spin rotation**.
- As the reverse field increases, **domain walls begin to move**, but only after overcoming pinning barriers.

The field required to reduce the magnetization to zero is the **coercive field** H_c, which is primarily determined by the strength of domain wall pinning.

Summary

Different regions of the hysteresis loop are dominated by different mechanisms:

Region of loop	Dominant mechanism
Initial slope	Domain wall motion (easy, reversible)
Mid region	Domain wall motion (pinned, irreversible)
Near saturation	Spin rotation
High field	Saturated state
Reversal near H_c	Domain wall depinning

Thus, hysteresis reflects the interplay between domain wall dynamics, spin rotation, and pinning effects in real materials.

9.4 Irreversibility and coercivity

Hysteresis arises because domain wall motion is not perfectly reversible. Defects, impurities, and lattice imperfections act as **pinning centers** that impede the motion of domain walls. As a result, additional energy is required to move domain walls, leading to hysteresis and a finite coercive field. The strength of pinning determines the magnetic hardness of the material:

- **Soft ferromagnets**: small H_c, narrow hysteresis loop.
- **Hard ferromagnets**: large H_c, wide hysteresis loop.

9.5 Connection to microscopic theory

The existence of magnetic domains and hysteresis reflects a competition between several energy scales:

- **Exchange energy**: favors parallel alignment of spins.
- **Magnetostatic energy**: favors formation of domains to reduce stray fields.
- **Anisotropy energy**: favors alignment along specific crystallographic directions.
- **Domain wall energy**: penalizes spatial variation of magnetization.

The domain wall width is determined by the balance between exchange and anisotropy,

$$\delta \sim \sqrt{\frac{A}{K}}, \tag{81}$$

The constant K is the magnetic anisotropy energy density, which arises from spin–orbit coupling and determines the preferred direction of magnetization. The exchange stiffness A is related to the spin-wave stiffness D introduced earlier; Both originate from the same microscopic exchange interaction, but appear in real-space and momentum-space descriptions, respectively. Intuitively, A is a measure of the cost to bend magnetization in space.

9.6 Energy loss and applications

The area of the hysteresis loop corresponds to the energy dissipated per cycle:

$$W = \oint H \, dM. \tag{82}$$

This energy loss is important in applications such as transformers and magnetic storage devices. Materials with small hysteresis losses are used in transformer cores, while materials with large coercivity are used for permanent magnets.

9.7 Physical interpretation

Hysteresis demonstrates that ferromagnets are inherently **non-equilibrium systems** on experimental time scales. The magnetization depends not only on the instantaneous external field but also on the history of the system. This behavior arises from the complex energy landscape associated with domain structures and pinning effects. Thus, while the Heisenberg model and spin-wave theory describe equilibrium properties, hysteresis reflects the dynamics of domain evolution in real materials.

10 Magnetization Dynamics: Landau–Lifshitz–Gilbert Equation

So far, we have described the *equilibrium properties* of ferromagnets using the Heisenberg model and micromagnetic energy. We now turn to the **dynamics of magnetization**, which governs how the system evolves in time under an effective magnetic field.

10.1 Torque on a magnetic moment

A magnetic moment $\boldsymbol{\mu}$ in a magnetic field $\mathbf{B}$ experiences a torque

$$\boldsymbol{\tau} = \boldsymbol{\mu} \times \mathbf{B}. \tag{83}$$

Using the relation $\boldsymbol{\mu} = -\gamma \mathbf{S}$, where γ is the gyromagnetic ratio, the equation of motion becomes

$$\frac{d\mathbf{S}}{dt} = -\gamma \mathbf{S} \times \mathbf{B}. \tag{84}$$

In a continuous medium, this translates into an equation for the magnetization $\mathbf{M}(\mathbf{r}, t)$,

$$\frac{d\mathbf{M}}{dt} = -\gamma \mathbf{M} \times \mathbf{H}_{\text{eff}}. \tag{85}$$

This describes **precession** of magnetization around the effective field.

10.2 Effective magnetic field

The effective field is obtained from the variation of the total energy:

$$\mathbf{H}_{\text{eff}} = -\frac{1}{\mu_0} \frac{\delta E}{\delta \mathbf{M}}. \tag{86}$$

It includes contributions from all micromagnetic energy terms:

- Exchange field
- Anisotropy field
- External field
- Demagnetizing field

Thus, $\mathbf{H}_{\text{eff}}$ encodes all interactions discussed previously.

10.3 Landau–Lifshitz equation

The precession equation alone conserves energy and cannot describe relaxation toward equilibrium. To include dissipation, Landau and Lifshitz introduced a phenomenological damping term:

$$\frac{d\mathbf{M}}{dt} = -\gamma \mathbf{M} \times \mathbf{H}_{\text{eff}} - \lambda \mathbf{M} \times (\mathbf{M} \times \mathbf{H}_{\text{eff}}), \tag{87}$$

where λ is a damping parameter.
The second term drives $\mathbf{M}$ toward alignment with $\mathbf{H}_{\text{eff}}$.

10.4 Gilbert form of damping

A more commonly used form is the **Landau–Lifshitz–Gilbert (LLG) equation**,

$$\frac{d\mathbf{M}}{dt} = -\gamma \mathbf{M} \times \mathbf{H}_{\text{eff}} + \frac{\alpha}{M_s} \mathbf{M} \times \frac{d\mathbf{M}}{dt}, \tag{88}$$

where α is the **Gilbert damping constant**.
Rewriting this gives

$$\frac{d\mathbf{M}}{dt} = -\frac{\gamma}{1+\alpha^2} \left[\mathbf{M} \times \mathbf{H}_{\text{eff}} + \frac{\alpha}{M_s} \mathbf{M} \times (\mathbf{M} \times \mathbf{H}_{\text{eff}}) \right]. \tag{89}$$

10.5 Physical interpretation

The LLG equation contains two distinct terms:

- **Precession term** $(-\gamma \mathbf{M} \times \mathbf{H}_{\text{eff}})$
  - causes magnetization to rotate around the field
  - conserves energy
- **Damping term**
  - aligns $\mathbf{M}$ with $\mathbf{H}_{\text{eff}}$
  - dissipates energy

Thus, magnetization follows a **spiral trajectory** toward equilibrium.

10.6 Connection to hysteresis

The LLG equation provides a dynamical basis for hysteresis:

- Domain wall motion is governed by LLG dynamics under pinning forces.
- Spin rotation near saturation corresponds to coherent LLG evolution.
- Energy dissipation (loop area) arises from damping (α).

Thus, hysteresis reflects **non-equilibrium solutions** of the LLG equation.

10.7 Characteristic time scale

The precession frequency is

$$\omega = \gamma H_{\text{eff}}. \tag{90}$$

Typical values:

- GHz range for laboratory magnetic fields
- ultrafast dynamics in nanomagnets and spintronic devices

10.8 Small-angle dynamics and spin waves

Linearizing the LLG equation around a uniform magnetization direction recovers the spin-wave dispersion derived earlier.
Thus:

- Heisenberg model → static exchange
- Spin-wave theory → normal modes
- LLG equation → full time-dependent dynamics

10.9 Summary

The Landau–Lifshitz–Gilbert equation provides a unified description of magnetization dynamics:

- describes precession and damping of spins
- connects microscopic interactions to macroscopic dynamics
- underlies modern magnetism, including spintronics and magnetic switching

It forms the foundation for understanding dynamic phenomena such as ferromagnetic resonance, domain wall motion, and ultrafast magnetization switching.

A Orbital Quenching in Transition Metals

In isolated atoms the electronic states possess spherical symmetry and are eigenstates of orbital angular momentum. In crystalline solids, however, the orbital contribution to the magnetic moment of most $3d$ transition metals is strongly suppressed. This phenomenon is known as *orbital quenching*. In this appendix we give a simple demonstration of how this occurs.

A.1 Atomic orbitals and angular momentum

In a central potential the electron wavefunction separates as

$$\psi(r, \theta, \phi) = R(r) Y_{\ell m}(\theta, \phi), \tag{91}$$

where $Y_{\ell m}$ are spherical harmonics. These functions are eigenstates of the angular momentum operator,

$$L_z Y_{\ell m} = m\hbar Y_{\ell m}. \tag{92}$$

For d orbitals we have $\ell = 2$ and therefore five degenerate states

$$m = -2, -1, 0, 1, 2. \tag{93}$$

Because these states are degenerate, electrons can occupy states with well-defined orbital angular momentum and therefore carry an orbital magnetic moment.

A.2 Phase winding and orbital angular momentum

The spherical harmonics contain an azimuthal phase factor

$$Y_{\ell m}(\theta, \phi) \propto e^{im\phi}. \tag{94}$$

This factor means that the complex phase of the wavefunction changes as one moves around the nucleus in the azimuthal direction. If the electron circles the nucleus once,

$$\phi \to \phi + 2\pi, \tag{95}$$

the wavefunction transforms as

$$\psi \to e^{i2\pi m} \psi. \tag{96}$$

Thus the phase changes by

$$\Delta\text{phase} = 2\pi m. \tag{97}$$

This behaviour is called *phase winding*. The wavefunction winds m times around the nucleus when the electron completes one full loop.
The connection to angular momentum follows from

$$L_z = -i\hbar \frac{\partial}{\partial \phi}. \tag{98}$$

Acting on the phase factor gives

$$L_z e^{im\phi} = -i\hbar \frac{\partial}{\partial \phi} e^{im\phi} = m\hbar e^{im\phi}. \tag{99}$$

Thus the orbital angular momentum is directly associated with the azimuthal phase winding of the wavefunction.

A.3 Circulating probability current

Phase winding produces a circulating probability current. The quantum probability current density is

$$\mathbf{j} = \frac{\hbar}{m_e} \operatorname{Im} \left(\psi^* \nabla \psi \right). \tag{100}$$

For a wavefunction containing the factor $e^{im\phi}$,

$$\nabla \psi \propto \frac{im}{r} \hat{\phi} \psi, \tag{101}$$

so that

$$\mathbf{j} \propto m\hat{\phi}. \tag{102}$$

Thus the electron probability flows azimuthally around the nucleus. This circulating current produces an orbital magnetic moment

$$\boldsymbol{\mu}_L = -\mu_B \mathbf{L}. \tag{103}$$

A.4 Real d orbitals in solids

In crystalline solids the five d orbitals are usually expressed as real orbitals

$$d_{xy},\ d_{xz},\ d_{yz},\ d_{x^2-y^2},\ d_{z^2}. \tag{104}$$

These orbitals are linear combinations of spherical harmonics. For example

$$d_{x^2-y^2} = \frac{1}{\sqrt{2}} \left(Y_{2,2} + Y_{2,-2} \right), \tag{105}$$

$$d_{xy} = \frac{1}{i\sqrt{2}} \left(Y_{2,2} - Y_{2,-2} \right). \tag{106}$$

Substituting the phase factors gives

$$Y_{2,2} + Y_{2,-2} \propto e^{i2\phi} + e^{-i2\phi} = 2\cos(2\phi). \tag{107}$$

The complex phases cancel, leaving a purely real wavefunction with no azimuthal phase winding.

A.5 Expectation value of angular momentum

Consider the orbital

$$d_{x^2-y^2} = \frac{1}{\sqrt{2}} \left(Y_{2,2} + Y_{2,-2} \right). \tag{108}$$

Applying the angular momentum operator,

$$L_z Y_{2,m} = m\hbar Y_{2,m}, \tag{109}$$

gives

$$L_z d_{x^2-y^2} = \frac{1}{\sqrt{2}} \left(2\hbar Y_{2,2} - 2\hbar Y_{2,-2} \right). \tag{110}$$

The expectation value becomes

$$\langle L_z \rangle = 0. \tag{111}$$

Similarly

$$\langle L_x \rangle = \langle L_y \rangle = 0, \tag{112}$$

so that

$$\langle \mathbf{L} \rangle = 0. \tag{113}$$

Thus electrons occupying these real orbitals do not carry orbital angular momentum.

A.6 Role of the crystal field

In transition metal solids the surrounding ions generate an anisotropic electrostatic potential known as the crystal field. This potential removes the degeneracy of the atomic d levels and selects orbitals that are spatially oriented relative to the ligands.
For example, in an octahedral crystal field

$$t_{2g} = (d_{xy}, d_{xz}, d_{yz}), \qquad e_g = (d_{x^2-y^2}, d_{z^2}). \tag{114}$$

Because these orbitals are real spatial orbitals fixed relative to the lattice, the degeneracy required to form complex combinations with phase winding is removed. Consequently, the orbital angular momentum becomes quenched.
For this reason, the magnetic moments of most $3d$ transition metals are well approximated by the *spin-only* expression

$$\mu \approx g\sqrt{S(S+1)}\,\mu_B, \tag{115}$$

with $g \approx 2$.

B Mermin–Wagner Theorem

The Mermin–Wagner theorem states that continuous symmetries cannot be spontaneously broken at finite temperature in one- or two-dimensional systems with sufficiently short-range interactions. As a consequence, long-range magnetic order is forbidden in strictly one- and two-dimensional isotropic Heisenberg magnets at any finite temperature.
This result was first established by N. D. Mermin and H. Wagner (Phys. Rev. Lett. 17, 1133 (1966)).

B.1 Statement of the theorem

Consider a system with a continuous symmetry such as the rotational symmetry of the Heisenberg Hamiltonian

$$H = -J \sum_{\langle ij \rangle} \mathbf{S}_i \cdot \mathbf{S}_j. \tag{116}$$

The Mermin–Wagner theorem states that for systems with dimension

$$d \leq 2 \tag{117}$$

and short-range interactions, spontaneous long-range order associated with the breaking of a continuous symmetry cannot occur at finite temperature.
In particular,

- No ferromagnetic or antiferromagnetic long-range order exists in a 1D or 2D isotropic Heisenberg magnet at $T > 0$.
- Long-range order can occur only at $T = 0$.

B.2 Physical origin: low-energy spin waves

The physical origin of the theorem lies in the large number of low-energy long-wavelength fluctuations present in low-dimensional systems.
Consider a ferromagnet with magnetization aligned along the z direction. Low-energy excitations correspond to slowly varying rotations of the spin direction. These excitations are spin waves (magnons).
For a Heisenberg ferromagnet, the spin-wave energy is

$$\epsilon(\mathbf{k}) = Dk^2, \tag{118}$$

where D is the spin stiffness.

B.3 Thermal population of spin waves

At finite temperature, the number of thermally excited magnons is

$$n_{\mathbf{k}} = \frac{1}{e^{\beta \epsilon_{\mathbf{k}}} - 1}. \tag{119}$$

Each magnon reduces the magnetization by one unit of spin. The reduction in magnetization due to thermal fluctuations is therefore

$$\Delta M \propto \int \frac{d^d k}{(2\pi)^d} \frac{1}{e^{\beta D k^2} - 1}. \tag{120}$$

For small k we can approximate

$$n_{\mathbf{k}} \approx \frac{T}{D k^2}. \tag{121}$$

Thus the magnetization correction behaves as

$$\Delta M \propto \int \frac{d^d k}{k^2}. \tag{122}$$

B.4 Infrared divergence in low dimensions

The behaviour of this integral depends on the spatial dimension.

Three dimensions

$$\Delta M \propto \int_0 dk\, k \tag{123}$$

which converges. Therefore long-range order survives at finite temperature.

Two dimensions

$$\Delta M \propto \int_0 \frac{dk}{k}. \tag{124}$$

This integral diverges logarithmically as $k \to 0$. Long-wavelength fluctuations destroy the magnetization.

One dimension

$$\Delta M \propto \int_0 \frac{dk}{k^2}, \tag{125}$$

which diverges even more strongly.
Thus in $d \leq 2$ the thermal population of long-wavelength spin waves diverges and completely destroys long-range order.

B.5 Consequences

The theorem implies that strictly two-dimensional isotropic Heisenberg magnets cannot exhibit spontaneous magnetic order at finite temperature. However, several mechanisms can stabilize magnetic order in real materials:

- Magnetic anisotropy (breaking continuous symmetry)
- Dipolar interactions
- Interlayer coupling
- Finite sample size

For example, if an easy-axis anisotropy reduces the symmetry from continuous $SU(2)$ to discrete Ising symmetry, long-range order becomes possible even in two dimensions.

B.6 Relation to two-dimensional magnetism

The Mermin–Wagner theorem plays an important role in modern condensed matter physics, particularly in the study of two-dimensional materials. In systems such as monolayer magnetic crystals or ultra-thin magnetic films, long-range order can occur only when anisotropy or spin–orbit coupling breaks the continuous rotational symmetry. This explains why magnetic ordering in atomically thin materials such as CrI_3 or Fe_3GeTe_2 relies on strong magnetic anisotropy.